JAERI-Research
96-064

CONCEPTUAL DESIGN OF IFMIF ACCELERATOR RF SYSTEMS

December 1996

Michael A. CHERNOGUBOVSKY* and
Masayoshi SUGIMOTO

日本原子力研究所
Japan Atomic Energy Research Institute

本レポートは，日本原子力研究所が不定期に公刊している研究報告書です。
入手の問合わせは，日本原子力研究所研究情報部研究情報課（〒319-11 茨城県那珂郡東海村）あて，お申し越しください。なお，このほかに財団法人原子力弘済会資料センター（〒319-11 茨城県那珂郡東海村日本原子力研究所内）で複写による実費頒布をおこなっております。

This report is issued irregularly.
Inquiries about availability of the reports should be addressed to Research Information Division, Department of Intellectual Resources, Japan Atomic Energy Research Institute, Tokai-mura, Naka-gun, Ibaraki-ken 319-11, Japan.

編集兼発行　日本原子力研究所
印　　刷　㈱原子力資料サービス

Conceptual Design of IFMIF Accelerator RF Systems

Michael A. CHERNOGUBOVSKY* and Masayoshi SUGIMOTO

Department of Reactor Engineering
Tokai Research Establishment
Japan Atomic Energy Research Institute
Tokai-mura, Naka-gun, Ibaraki-ken

(Received November 13, 1996)

The following three items are considered under the IFMIF conceptual design activities. (1) The electrodynamical properties of the segmented RFQ are analyzed.(2) Directional selective coupling is applied for RF systems design of the RFQ. This can exclude the different type transmission line long feeders and can eliminate excitation of the undesirable modes under the intense beam acceleration. The matching between RF source and accelerating structures is accomplished. RF signals to support control system are produced. (3) The structure fine tuning method using electro-optical principle is devised.

Keywords: Resonator, Mode, RFQ, DTL, Accelerator, Directional Coupler

---

* Research Fellow

ＩＦＭＩＦ加速器高周波システムの概念設計

日本原子力研究所東海研究所原子炉工学部
Michael A. CHERNOGUBOVSKY* ・杉本　昌義

（1996年11月13日受理）

ＩＦＭＩＦ概念設計活動の一環として加速器システムに関する以下の３点について考察した。(1)基本設計に採用されたセグメント型ＲＦＱの電気力学的性質を解析し，セグメント間のギャップ領域において問題となる過度な電場強度及びビームダイナミクスへの悪影響を最小限に押さえるための電極形状を提案した。(2)ＲＦＱへの高周波の供給に方向性選択結合器を適用する設計を提案した。この方法により高周波伝送系で使われる伝送線路長の種類が少なくなり，大強度ビーム加速で問題となる不要なモードの励起を押さえられる。また高周波源と加速空洞との整合がよくとれるようになり，高周波制御に使用可能な信号も取出せる。(3)空洞内に挿入した光半導体に外部から光を当てることで空洞内部の電磁場に擾乱を加えその影響を測定する技術を応用したＲＦＱの精密な同調方法の適用を提案した。

東海研究所：〒319-11　茨城県那珂郡東海村白方白根２－４
＊原研リサーチフェロー

Contents

目　　次

1. Introduction

The main specifications of the IFMIF deuteron linac are 40 MeV energy and 125 mA beam intensity with continuous-wave (CW) operating conditions [1]. This accelerator requires some careful considerations on the accelerating structures and the RF system designs. There are several generic issues such as the development of the high power feeders to the accelerating structures and the matching problem between the RF sources and the couplers. For designing of the four-vane RFQ which is used for initial acceleration up to 8 MeV, both the elimination of the undesirable modes and the precise tuning of the structure become important [2,3]. As the advanced segmentation principle [4-6] is applied for relatively long RFQ structure design, special features of the operating mode must be also considered. The report presents the RF system conception to obtain simultaneous solution of these problems.

2. Segmented RFQ operating mode

2.1 General field properties in the gap region

According to the method described in [7] all quadrupole modes of RFQ are derived by the electric (i.e. ideal metal) walls setting in the symmetry planes (II′ and II″ in Fig. 1). Under the segmentation [4-6] the longitudinally equidistant arrangement of two identical cuts of the vanes is provided. This yields the symmetry conditions for electric or magnetic walls placing in these cut's midpoint ($z1 = 0$ in Fig. 1a). The electric walls, shown by a shaded circle in Fig. 1a, derive operating mode[1]. Due to this property, it is possible to consider the fields of any RFQ segments separately.

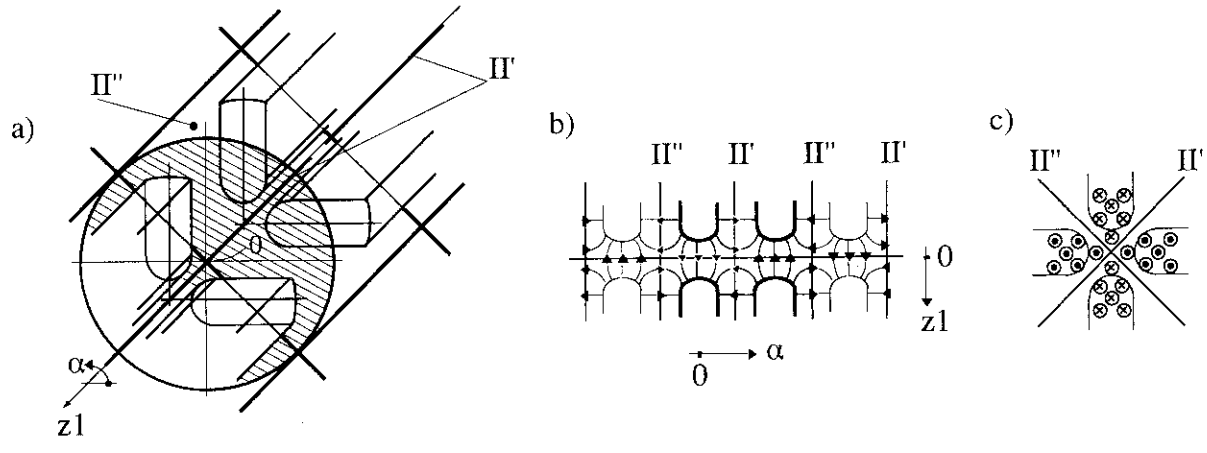

Fig. 1. (a) Inter-segment gap in segmented RFQ (electric walls are marked by thick lines); (b) electric field in radial cross-section, and (c) in $z1 = 0$ plain.

The mode field properties do not depend on presence of thin diaphragm at the segment

[1] It is indicated by the description of magnetic field configuration in undercuts region in [4,5].

1. Introduction

The main specifications of the IFMIF deuteron linac are 40 MeV energy and 125 mA beam intensity with continuous-wave (CW) operating conditions [1]. This accelerator requires some careful considerations on the accelerating structures and the RF system designs. There are several generic issues such as the development of the high power feeders to the accelerating structures and the matching problem between the RF sources and the couplers. For designing of the four-vane RFQ which is used for initial acceleration up to 8 MeV, both the elimination of the undesirable modes and the precise tuning of the structure become important [2,3]. As the advanced segmentation principle [4-6] is applied for relatively long RFQ structure design, special features of the operating mode must be also considered. The report presents the RF system conception to obtain simultaneous solution of these problems.

2. Segmented RFQ operating mode

2.1 General field properties in the gap region

According to the method described in [7] all quadrupole modes of RFQ are derived by the electric (i.e. ideal metal) walls setting in the symmetry planes (II′ and II″ in Fig. 1). Under the segmentation [4-6] the longitudinally equidistant arrangement of two identical cuts of the vanes is provided. This yields the symmetry conditions for electric or magnetic walls placing in these cut's midpoint ($z1 = 0$ in Fig. 1a). The electric walls, shown by a shaded circle in Fig. 1a, derive operating mode[1]. Due to this property, it is possible to consider the fields of any RFQ segments separately.

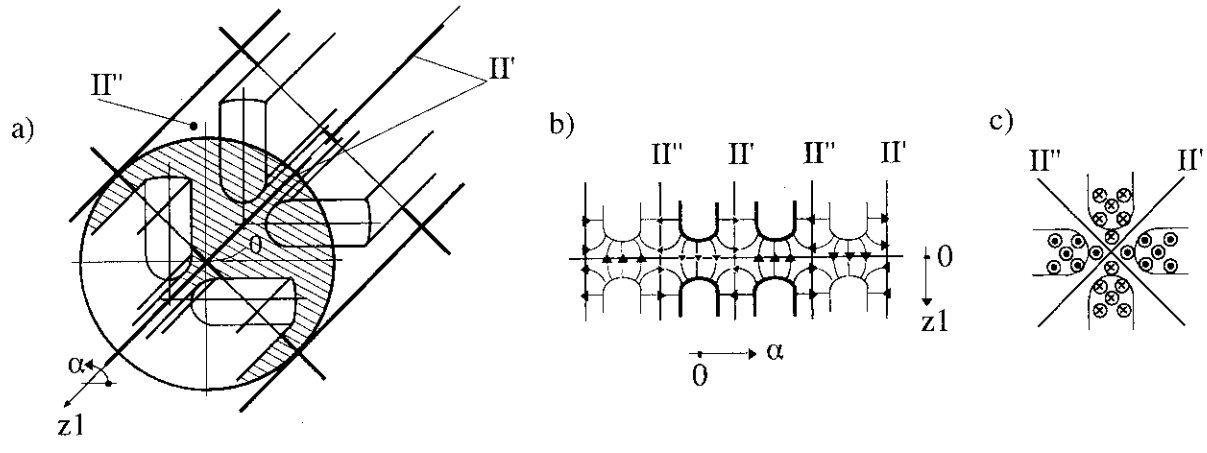

Fig. 1. (a) Inter-segment gap in segmented RFQ (electric walls are marked by thick lines); (b) electric field in radial cross-section, and (c) in $z1 = 0$ plain.

The mode field properties do not depend on presence of thin diaphragm at the segment

[1] It is indicated by the description of magnetic field configuration in undercuts region in [4,5].

boundary. The diaphragm is described as the "coupling plate" in [4], and its shape has no effect to the operating mode. Whereas, the properties of the other mode[2], which is derived by the magnetic walls setting, will be strongly affected by its shape. In contrast, the influence of the gap size on separation of the mode frequencies is rather small, vanishing for the longer segments[3]. The operating mode field distribution is obtained by the radial propagation of quasi-TEM wave in the four identical short-circuited inhomogeneous coaxial (quasi-rectangular) transmission lines, terminated by the capacitive loads between the electrode end and inter-wall corner. Fig. 1.b shows the field pattern at the segment gap region in the longitudinal axis $z1$ and azimuthal angle α coordinates in radial cross-section. According to the TEM wave property, the inter-gap voltage between the vane ends is independent to the gap width and equal to the voltages between the adjacent vanes of the segment in any radial cross-section. The field pattern represented in the midplane of the segment gap is shown in Fig. 1c. Their signs are changed in each quadrant separated by the symmetry planes, and the longitudinal components only exist in the midplane.

In the real case, the symmetry is not exact and the electric wall may not have a plane surface. It may be shifted from the midplane position ($z1 = 0$ in Fig. 1a,b). The modulation of the electrode ends will deform right angle between the symmetry planes II′ and II″ walls near the corner. The field patterns shown in Fig. 1b,c are no longer completely symmetrical. Nevertheless, the above-mentioned properties will remain as before.

Minimal distortion of proper beam dynamics by the gap field can be obtained by symmetrical field distribution on Fig. 1c, that leads to the gap design in electrodes without modulation region: p intervals as shown on Fig. 2a.

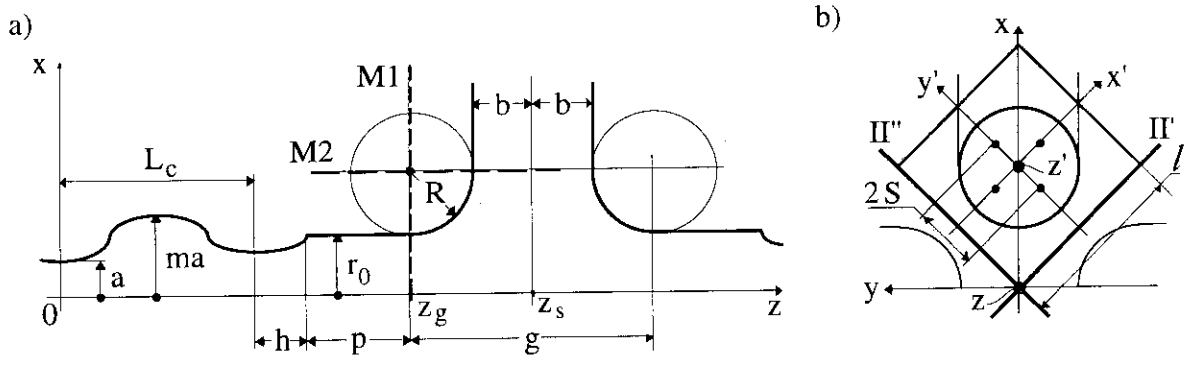

Fig. 2. (a) Possible shapes of the gap forming elements, (b) $z = z_g$ cross-section.

The gap width is desired to be minimized, however, it is constrained by the allowed electric strength[4]. The same strength as in the main RFQ part can be achieved by employing the

[2]This mode is considered as the operating one in [6].

[3]Modes will be in existence even for the greater than wavelength size, when coupling between the ends of the vanes is not "capacitative" [4,5].

[4]The width in [5] seems to be excessively small.

same inter-surface distance with spherical shape of the vane corners and rounded edges. The possible shape of the gap region is indicated in Fig. 2a, where the half inter-gap width is given by $b = ((r_0 + R)/\sqrt{2}) - R$. In this case the focusing quadrupoles will be added before and after the gap where the field is substantially different from the ordinary RFQ one. The intervals, p and h, of each gap region should be adjusted to the actual electrode modulations and accelerating conditions in the gap positions.

2.2 Gap field

Transverse field orientation in p interval and the beam aperture bounded region consideration allow to place magnetic walls $M1$ and $M2$ (Fig. 2a). Therefore, the gap field will coincide with the sphere in cube field in $x \leq r_0 + R$, $z_g \leq z \leq z_s$ space (Fig. 2a,b). Conventional electrostatic approximation of this field under equality of the sphere potential A_0 to uninterrupted by the gap electrode potential A_e at $z = z_g$ point (refer to zero potential of II′, II″ walls) yields the gap field at symmetrical continuous extension into other gap's spaces.

Sphere in cube electrostatic problem solution by mirror image's method gives an advantage, since the result will already have just right continuation for all the gap field. In local coordinates x', y', z' (Fig. 2b) a charge q, located inside the cube in x'_0, y'_0, z'_0 point, sets up the potential

$$\varphi(x', y', z') = \frac{q}{4\pi\varepsilon_0 l} \cdot \Phi(x'_{0N}, y'_{0N}, z'_{0N}; x'_N, y'_N, z'_N); \tag{1}$$

where $\Phi(x'_{0N}, y'_{0N}, z'_{0N}; x'_N, y'_N, z'_N) =$

$$\sum_{\substack{-\infty \\ (i)}}^{+\infty} \sum_{\substack{-\infty \\ (j)}}^{+\infty} \sum_{\substack{-\infty \\ (n)}}^{+\infty} \frac{(-1)^{i+j+n}}{\sqrt{(x'_N - i - (-1)^i \cdot x'_{0N})^2 + (y'_N - j - (-1)^j \cdot y'_{0N})^2 + (z'_N - n - (-1)^n \cdot z'_{0N})^2}},$$

all linear dimensions are normalized to l and denoted by index N, e.g., $x'_N = x'/l$. For satisfaction of the sphere surface conditions consider the normalized potential Φ_M of symmetrical set: one charge $6q \cdot \eta$ in the center of the sphere with six equal charges q, disposed symmetrically on the axes at S distance (Fig. 2b):

$$\Phi_M(x'_N, y'_N, z'_N) = 6\eta \cdot \Phi(0, 0, 0; x'_N, y'_N, z'_N) + \Phi_6(S_N, x'_N, y'_N, z'_N), \tag{2}$$

$$\begin{aligned} \Phi_6(S_N, x'_N, y'_N, z'_N) = {} & \Phi(+S_N, 0, 0; x'_N, y'_N, z'_N) + \Phi(-S_N, 0, 0; x'_N, y'_N, z'_N) + \\ & \Phi(0, +S_N, 0; x'_N, y'_N, z'_N) + \Phi(0, -S_N, 0; x'_N, y'_N, z'_N) + \\ & \Phi(0, 0, +S_N; x'_N, y'_N, z'_N) + \Phi(0, 0, -S_N; x'_N, y'_N, z'_N). \end{aligned} \tag{3}$$

Equality of Φ_M to Ψ_0 in three points:

$$P_1 = \{R_N, 0, 0\}, \quad P_2 = \{R_N/\sqrt{2}, R_N/\sqrt{2}, 0\}, \quad P_3 = \{R_N/\sqrt{3}, R_N/\sqrt{3}, R_N/\sqrt{3}\},$$

yields the equation for S_N value determination

$$\Phi_6(0,P_1)\cdot\Big(\Phi_6(S_N,P_3) - \Phi_6(S_N,P_2)\Big) + \Phi_6(0,P_2)\cdot\Big(\Phi_6(S_N,P_1) - \Phi_6(S_N,P_3)\Big) + \Phi_6(0,P_3)\cdot\Big(\Phi_6(S_N,P_2) - \Phi_6(S_N,P_1)\Big) = 0 \tag{4}$$

since $6\Phi(0,0,0;x'_N,y'_N,z'_N) = \Phi_6(0,x'_N,y'_N,z'_N)$, and determines Ψ_0 and η values

$$\Psi_0 = \frac{\Phi_6(S_N,P_1)\cdot\Phi_6(0,P_2) - \Phi_6(S_N,P_2)\cdot\Phi_6(0,P_1)}{\Phi_6(0,P_2) - \Phi_6(0,P_1)}, \tag{5}$$

$$\eta = \frac{\Phi_6(S_N,P_1) - \Phi_6(S_N,P_2)}{\Phi_6(0,P_2) - \Phi_6(0,P_1)}; \tag{6}$$

the form (2) evenness and permutative invariance refer to x'_N, y'_N, z'_N will give the same Ψ_0 potential in all other symmetrically disposed points. For $R = r_0$ case (one of the optimal cases, [8]) the unique root of Eq. (4) is $S_N = 0.14505$; $\eta = -0.176856$, $\Psi_0 = 5.3304$. Real accuracy of this method is determined at analysis of $\Phi_M = \Psi_0$ equipotential shape in the varying radius $R_{Ne}(x'_N, y'_N)$ form, in Fig. 3 the deviation $(R_N - R_{Ne}(x'_N, y'_N))/R_N$ is shown.

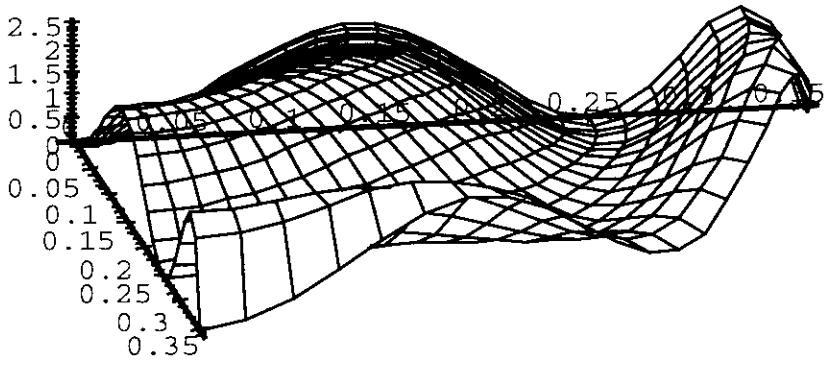

Fig. 3. Radius normalized error $\times 10^4$ in a quadrant space ($R{=}r_0, R_N{=}1/2\sqrt{2}$).

The error does not exceed $2.5\cdot10^{-4}$, for $R = 8$ mm it corresponds to $2\,\mu$m, that is less than fabrication tolerance; the cube walls boundary conditions satisfaction ensures exact field configuration in the beam aperture.

2.3 PARMTEQ input data

Within the accuracy of the RFQ field approximation in PARMTEQ code [9], the desired equivalence of $A_e = V/2$ to $A_0 = \frac{q}{4\pi\varepsilon_0 l}\Psi_0$ determines q value. The potential Φ_M transformation to PARMTEQ coordinates x, y, z (Fig. 2):

$$x'_N = \frac{x-y}{l\sqrt{2}} - \frac{1}{2}, \quad y'_N = \frac{x+y}{l\sqrt{2}} - \frac{1}{2}, \quad z'_N = \frac{z-z_g}{l},$$

yields the result for electric field components:

$$E_u = \frac{-V}{2\sqrt{2}\Psi_0 l}\cdot\sum_{(i)}^{+\infty}\sum_{(j)}^{+\infty}\sum_{(n)}^{+\infty}(-1)^{i+j+n}\Big(D_u(S_N,0,0)+D_u(-S_N,0,0)+$$
$$D_u(0,S_N,0)+D_u(0,-S_N,0)+D_u(0,0,S_N)+$$
$$D_u(0,0,-S_N)+6\eta D_u(0,0,0)\Big), \qquad u=x,y,z; \tag{7}$$

where

$$D_x(\nu_1,\nu_2,\nu_3,) = (1+i+(-1)^i\cdot\nu_1+j+(-1)^j\cdot\nu_2-\frac{x\sqrt{2}}{l})\cdot D^{-\frac{3}{2}},$$
$$D_y(\nu_1,\nu_2,\nu_3,) = (-i-(-1)^i\cdot\nu_1+j+(-1)^j\cdot\nu_2-\frac{y\sqrt{2}}{l})\cdot D^{-\frac{3}{2}},$$
$$D_z(\nu_1,\nu_2,\nu_3,) = \sqrt{2}\cdot(n+(-1)^n\cdot\nu_3-\frac{z-z_g}{l})\cdot D^{-\frac{3}{2}};$$

and

$$D = \Big(\frac{x-y}{l\sqrt{2}}-\frac{1}{2}-i-(-1)^i\cdot\nu_1\Big)^2+$$
$$\Big(\frac{x+y}{l\sqrt{2}}-\frac{1}{2}-j-(-1)^j\cdot\nu_2\Big)^2+\Big(\frac{z-z_g}{l}-n-(-1)^n\cdot\nu_3\Big)^2.$$

So, accelerating bore field at L_c, h, p intervals (Fig. 2.a) is determined by (1) - (3) expressions in [9]; g field is defined by expression (7), multiplied by time-dependent factor $\sin\omega t$ or by $\sin z$ in accordance to PARMTEQ method (see Eq. (6) in [9]). In (7) expression the S_N parameter is the root of Eq. (4) and Ψ_0, η values are determined by formulae (5),(6). Deviation of potential (3) from zero on the cube walls determines desired finite numbers of terms in (1) and (7) sums for required precision[5].The result can be also used for consideration of end-walls regions in ordinary RFQ - expression (7) for $z \in [z_g, z_s]$.

3. Directional selective coupling RF system

Four drive loop feeding of RFQ segments gives the possibility for the directional selective coupling principle [7] application: the RF system contains three 3 dB directional couplers $D1 - D3$, equal length feeders $l_1 - l_4$ and $l_5 - l_6$ to attain equal amplitudes cophased excitation at equal coupling loops spaces in each segment; feeders-loops matching on operating mode results in full decoupling of matched loads $c1 - c3$ in Fig. 4. In the intense beam case the lowering of undesirable mode quality factors is effective, [7], so the "dipole stabilizer" rods (Fig. 1 in [4,5]) can be excluded.

For the longitudinally alternating quadrupole mode, the first and the third segment loops are to be fed as shown on Fig. 1 in [7], but the second segment loops must be replaced

[5]The best precision is obtained at $i \in [-(M+1); M], j \in [-(M+1); M], n \in [-N; N]$; $N \geq M$.

yields the result for electric field components:

$$E_u = \frac{-V}{2\sqrt{2}\Psi_0 l}\cdot\sum_{(i)=-\infty}^{+\infty}\sum_{(j)=-\infty}^{+\infty}\sum_{(n)=-\infty}^{+\infty}(-1)^{i+j+n}\Big(D_u(S_N,0,0)+D_u(-S_N,0,0)+$$
$$D_u(0,S_N,0)+D_u(0,-S_N,0)+D_u(0,0,S_N)+$$
$$D_u(0,0,-S_N)+6\eta D_u(0,0,0)\Big), \qquad u=x,y,z; \tag{7}$$

where

$$D_x(\nu_1,\nu_2,\nu_3,) = (1+i+(-1)^i\cdot\nu_1+j+(-1)^j\cdot\nu_2-\frac{x\sqrt{2}}{l})\cdot D^{-\frac{3}{2}},$$
$$D_y(\nu_1,\nu_2,\nu_3,) = (-i-(-1)^i\cdot\nu_1+j+(-1)^j\cdot\nu_2-\frac{y\sqrt{2}}{l})\cdot D^{-\frac{3}{2}},$$
$$D_z(\nu_1,\nu_2,\nu_3,) = \sqrt{2}\cdot(n+(-1)^n\cdot\nu_3-\frac{z-z_g}{l})\cdot D^{-\frac{3}{2}};$$

and

$$D = \Big(\frac{x-y}{l\sqrt{2}}-\frac{1}{2}-i-(-1)^i\cdot\nu_1\Big)^2+$$
$$\Big(\frac{x+y}{l\sqrt{2}}-\frac{1}{2}-j-(-1)^j\cdot\nu_2\Big)^2+\Big(\frac{z-z_g}{l}-n-(-1)^n\cdot\nu_3\Big)^2.$$

So, accelerating bore field at L_c, h, p intervals (Fig. 2.a) is determined by (1) – (3) expressions in [9]; g field is defined by expression (7), multiplied by time-dependent factor $\sin\omega t$ or by $\sin z$ in accordance to PARMTEQ method (see Eq. (6) in [9]). In (7) expression the S_N parameter is the root of Eq. (4) and Ψ_0, η values are determined by formulae (5),(6). Deviation of potential (3) from zero on the cube walls determines desired finite numbers of terms in (1) and (7) sums for required precision[5].The result can be also used for consideration of end-walls regions in ordinary RFQ – expression (7) for $z \in [z_g, z_s]$.

3. Directional selective coupling RF system

Four drive loop feeding of RFQ segments gives the possibility for the directional selective coupling principle [7] application: the RF system contains three 3 dB directional couplers $D1 - D3$, equal length feeders $l_1 - l_4$ and $l_5 - l_6$ to attain equal amplitudes cophased excitation at equal coupling loops spaces in each segment; feeders-loops matching on operating mode results in full decoupling of matched loads $c1 - c3$ in Fig. 4. In the intense beam case the lowering of undesirable mode quality factors is effective, [7], so the "dipole stabilizer" rods (Fig. 1 in [4,5]) can be excluded.

For the longitudinally alternating quadrupole mode, the first and the third segment loops are to be fed as shown on Fig. 1 in [7], but the second segment loops must be replaced

[5]The best precision is obtained at $i \in [-(M+1); M], j \in [-(M+1); M], n \in [-N; N]$; $N \geq M$.

into adjacent quadrants ("90 deg. slew" of all 4 loops); the nearest nonexcluded mode will be 9 longitudinal alternation's quadrupole. The directional couplers are realized on hybrid ring bridges. The installation of the bridges on each segment in three cross-sections excludes the majority of the different type long feeders. Bridge's realization on square coaxial line is the simplest, the central diameter will be about 0.8 m and there will be enough space between RFQ and the bridges for the square line with accordant electric strength; l_5 and l_6 feeders will be about 1 m length, and $l_1 \ldots l_4$ lengths – 20 cm, Fig. 4.

At the beam excitation the loads remain decoupled at operating mode but all undesirable modes are loaded on appropriate loads $c1 \ldots c3$ (the maximum loading is attained just at 3 dB transient attenuation of the couplers), while RF source is decoupled from these modes. In addition, the system assures RF source matching – e.g., in damage case in one of $l_1 \ldots l_4$ feeders or a loop breakdown the source feeder VSWR will be 1.4 (for vanishing length of $l_1 \ldots l_6$ feeders) and correlation of the high level signals $U1 - U3$ determines the damaged channel; in operating conditions any deviations from amplitude's equality of these low signals detect the operating mode asymmetry.

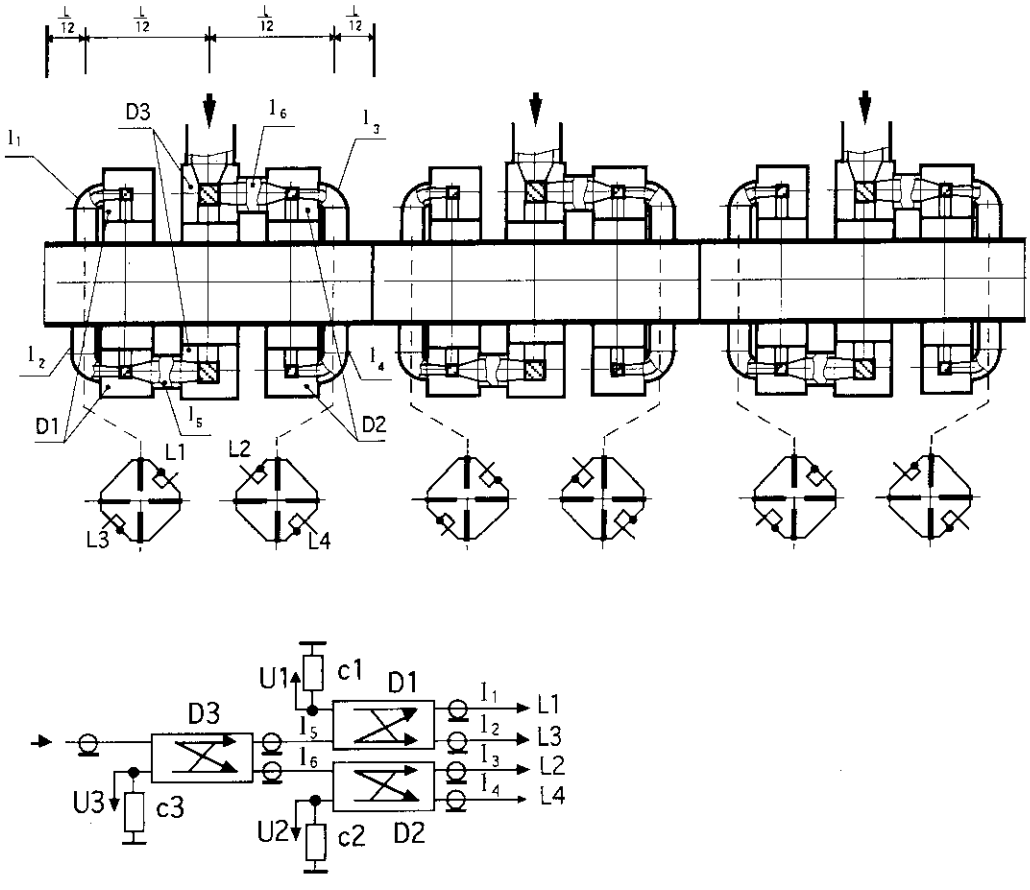

Fig. 4. RF system (not uniform longitudinal scale, L – total length).

Real system loops can not be absolutely equal, so the signals are in proportion to the resonator reflectance; $U1, U2$ and $U3$ phases form supporting for automatic control system phase-lock loop. For all that, any frequency differences between operating and eliminating

modes and even their coincidences are admissible[6] at least over the directional coupler's frequency band, the coupler central frequencies must be on the quadrupole mode resonance for additional loading minimization.

At experimental tests of the similar system [7] the undesirable mode levels are proved to be no more than −36 dB. The additional lowering (10−20 times) of the undesirable quality factors is obtained at the mismatched loads $c1 \ldots c3$; e.g., for short $l_1 \ldots l_4$ feeders the $c1, c2$ resistance must be greater than the wave impedance. The above-mentioned properties will remain as before except the source feeder matching in damage cases, however usually applied circulator will assure the matching. Computer simulation in [7] shows that a high degree of precision is not required for realization of the system components even for long $l_1 \ldots l_6$ feeders.

4. RF tuning

The strong advantage of [4,5] principle is possibility of fabrication of relatively short segment RFQs, those can be tuned separately under the real short-circuiting plates setting in the segment cut's midpoint $z1 = 0$, Fig. 1a. Accordant turn of the system Fig. 4 loops allows to excite any desired well-definable mode and the segment RFQ field symmetrization can be carried out by the degeneration property [7] of adjacent dipole modes; in this case "decoupled" tuning elements, analogous to "t" (see Fig. 1 in [7]) at the vane's undercuts are to be provided.

Determination of the quadrupole field symmetry axis positions (the [7] method accuracy is about 10 μm) gives the means for exact connection of the tuned segments; under the precise tuning method [10] the accuracy will be about 4 μm. The p spaces on Fig. 2a can be used for the installation of the master gauges or contact optical targets, which gives a convenient way for precise forming of the datum axis at RFQ segment field precise tuning and especially for the tuned segment axes setting into coincidence. The connected segments field symmetrization can be also examined by the dipole modes degeneration features and the exactness of each coupling loop tuning can be examined on quadrupole mode resonance at matched-loaded the rest eleven loops by VSWR=23 value verification.

Electro-optical precise measurements for desired RFQ vane ends modulation implementation can be combined with the axis determination procedure under equipotentials detecting principle by the means of doubled length lighted strip rotation on the round photosemiconductor plate, Fig. 1 in [10]. This principle at DTL tuning for precise measurements of acceleration period positions is realized by full lighting of the same round plate at minimal lighted − unlighted frequency deviation positions detecting inside the

[6]The indicated on Fig. 2 in [4,5] RFQ mode does not correlate with operating quadrupole [4,5] descriptions, so the idea of the longitudinal stability improvement by the stopband presence can not be interpreted; but Fig. 4 system provides this stability.

modes and even their coincidences are admissible[6] at least over the directional coupler's frequency band, the coupler central frequencies must be on the quadrupole mode resonance for additional loading minimization.

At experimental tests of the similar system [7] the undesirable mode levels are proved to be no more than −36 dB. The additional lowering (10−20 times) of the undesirable quality factors is obtained at the mismatched loads $c1 \ldots c3$; e.g., for short $l_1 \ldots l_4$ feeders the $c1, c2$ resistance must be greater than the wave impedance. The above-mentioned properties will remain as before except the source feeder matching in damage cases, however usually applied circulator will assure the matching. Computer simulation in [7] shows that a high degree of precision is not required for realization of the system components even for long $l_1 \ldots l_6$ feeders.

4. RF tuning

The strong advantage of [4,5] principle is possibility of fabrication of relatively short segment RFQs, those can be tuned separately under the real short-circuiting plates setting in the segment cut's midpoint $z1 = 0$, Fig. 1a. Accordant turn of the system Fig. 4 loops allows to excite any desired well-definable mode and the segment RFQ field symmetrization can be carried out by the degeneration property [7] of adjacent dipole modes; in this case "decoupled" tuning elements, analogous to "t" (see Fig. 1 in [7]) at the vane's undercuts are to be provided.

Determination of the quadrupole field symmetry axis positions (the [7] method accuracy is about 10 μm) gives the means for exact connection of the tuned segments; under the precise tuning method [10] the accuracy will be about 4 μm. The p spaces on Fig. 2a can be used for the installation of the master gauges or contact optical targets, which gives a convenient way for precise forming of the datum axis at RFQ segment field precise tuning and especially for the tuned segment axes setting into coincidence. The connected segments field symmetrization can be also examined by the dipole modes degeneration features and the exactness of each coupling loop tuning can be examined on quadrupole mode resonance at matched-loaded the rest eleven loops by VSWR=23 value verification.

Electro-optical precise measurements for desired RFQ vane ends modulation implementation can be combined with the axis determination procedure under equipotentials detecting principle by the means of doubled length lighted strip rotation on the round photosemiconductor plate, Fig. 1 in [10]. This principle at DTL tuning for precise measurements of acceleration period positions is realized by full lighting of the same round plate at minimal lighted − unlighted frequency deviation positions detecting inside the

[6]The indicated on Fig. 2 in [4,5] RFQ mode does not correlate with operating quadrupole [4,5] descriptions, so the idea of the longitudinal stability improvement by the stopband presence can not be interpreted; but Fig. 4 system provides this stability.

drift tubes. Autoreflection method with master gauges or contact optical targets fastening on the filament gives several micrometers accuracy at the tubes geometrical symmetry axis determination, and the field measurements in acceleration gaps and in ramp-field regions are carried out by thin longitudinal photosemiconductor cylinder with full lighting.

5. Conclusion

Analysis of segmented RFQ operating mode allowed to estimate the accelerating bore field distribution and the electrode possible shapes in inter-segment gap regions. It is necessary to prove the proper beam particle dynamics possibility for this quadrupole with the field, which is different from the ordinary RFQ field in the gaps[7]. Electrostatic approximation of these fields for computer simulation of the beam dynamics is proposed.

Conception of directional selective coupling principle application for segmented RFQ accelerating structure has been developed. The same conception can be applied for Alvarez-type DTL feeding or especially for H-type DTL and in all the cases when the undesirable mode problems become substantial.

The devised RFQ and DTL precise tuning methods are provided by the optical system under electro-optical principle application.

References

(1) Sugimoto M.:"Proc. of the 20th Linear Acc. Meeting in Japan", Free Electron Laser Research Institute, Inc. (FELI), 97 (1995).

(2) Howard D., Lancaster H.: IEEE Trans. Nucl. Sci., NS-30, 1446 (1983).

(3) Ueno A. et al.:"Proc. of 1990 Linear Accelerator Conf. Albuquerque, N.M., USA", Los Alamos Nat. Lab., 57 (1991).

(4) Young L. M.:private communication (1994).

(5) Young L. M.:"Proc. of the 1994 International Linac Conf. Tsukuba, Japan", National Laboratory for High Energy Physics (KEK), 178 (1994).

(6) Young L. M.:"Proc. of the 1993 Particle Accelerator Conf. Washington, USA", IEEE Inc., 3136 (1993).

(7) Chernogubovsky M. A., Kurchavy A. G., Liverovsky A. K.:"Portable 433 MHz RFQ Linac RF System", submitted to Nuc. Instr. Methods Phys. Res. A.

[7] Fig. 7 in [4] can not be considered as the dynamic simulation result, because any beam perturbations in gap's positions are absent.

drift tubes. Autoreflection method with master gauges or contact optical targets fastening on the filament gives several micrometers accuracy at the tubes geometrical symmetry axis determination, and the field measurements in acceleration gaps and in ramp-field regions are carried out by thin longitudinal photosemiconductor cylinder with full lighting.

5. Conclusion

Analysis of segmented RFQ operating mode allowed to estimate the accelerating bore field distribution and the electrode possible shapes in inter-segment gap regions. It is necessary to prove the proper beam particle dynamics possibility for this quadrupole with the field, which is different from the ordinary RFQ field in the gaps[7]. Electrostatic approximation of these fields for computer simulation of the beam dynamics is proposed.

Conception of directional selective coupling principle application for segmented RFQ accelerating structure has been developed. The same conception can be applied for Alvarez-type DTL feeding or especially for H-type DTL and in all the cases when the undesirable mode problems become substantial.

The devised RFQ and DTL precise tuning methods are provided by the optical system under electro-optical principle application.

References

(1) Sugimoto M.:"Proc. of the 20th Linear Acc. Meeting in Japan", Free Electron Laser Research Institute, Inc. (FELI), 97 (1995).

(2) Howard D., Lancaster H.: IEEE Trans. Nucl. Sci., NS-30, 1446 (1983).

(3) Ueno A. et al.:"Proc. of 1990 Linear Accelerator Conf. Albuquerque, N.M., USA", Los Alamos Nat. Lab., 57 (1991).

(4) Young L. M.:private communication (1994).

(5) Young L. M.:"Proc. of the 1994 International Linac Conf. Tsukuba, Japan", National Laboratory for High Energy Physics (KEK), 178 (1994).

(6) Young L. M.:"Proc. of the 1993 Particle Accelerator Conf. Washington, USA", IEEE Inc., 3136 (1993).

(7) Chernogubovsky M. A., Kurchavy A. G., Liverovsky A. K.:"Portable 433 MHz RFQ Linac RF System", submitted to Nuc. Instr. Methods Phys. Res. A.

[7] Fig. 7 in [4] can not be considered as the dynamic simulation result, because any beam perturbations in gap's positions are absent.

drift tubes. Autoreflection method with master gauges or contact optical targets fastening on the filament gives several micrometers accuracy at the tubes geometrical symmetry axis determination, and the field measurements in acceleration gaps and in ramp-field regions are carried out by thin longitudinal photosemiconductor cylinder with full lighting.

5. Conclusion

Analysis of segmented RFQ operating mode allowed to estimate the accelerating bore field distribution and the electrode possible shapes in inter-segment gap regions. It is necessary to prove the proper beam particle dynamics possibility for this quadrupole with the field, which is different from the ordinary RFQ field in the gaps[7]. Electrostatic approximation of these fields for computer simulation of the beam dynamics is proposed.

Conception of directional selective coupling principle application for segmented RFQ accelerating structure has been developed. The same conception can be applied for Alvarez-type DTL feeding or especially for H-type DTL and in all the cases when the undesirable mode problems become substantial.

The devised RFQ and DTL precise tuning methods are provided by the optical system under electro-optical principle application.

References

(1) Sugimoto M.:"Proc. of the 20th Linear Acc. Meeting in Japan", Free Electron Laser Research Institute, Inc. (FELI), 97 (1995).

(2) Howard D., Lancaster H.: IEEE Trans. Nucl. Sci., NS-30, 1446 (1983).

(3) Ueno A. et al.:"Proc. of 1990 Linear Accelerator Conf. Albuquerque, N.M., USA", Los Alamos Nat. Lab., 57 (1991).

(4) Young L. M.:private communication (1994).

(5) Young L. M.:"Proc. of the 1994 International Linac Conf. Tsukuba, Japan", National Laboratory for High Energy Physics (KEK), 178 (1994).

(6) Young L. M.:"Proc. of the 1993 Particle Accelerator Conf. Washington, USA", IEEE Inc., 3136 (1993).

(7) Chernogubovsky M. A., Kurchavy A. G., Liverovsky A. K.:"Portable 433 MHz RFQ Linac RF System", submitted to Nuc. Instr. Methods Phys. Res. A.

[7] Fig. 7 in [4] can not be considered as the dynamic simulation result, because any beam perturbations in gap's positions are absent.

(8) Kapchinsky I. M.:"Theory of Linear Resonant Accelerators", Energoisdat, Moscow, 240 (1982).

(9) Crandall K. R., Wangler T. P.:"AIP Conference Proceedings 177, New York, 1988", American Institute of Physics, 177, 22 (1988).

(10) Chernogubovsky M. A., Vorogushin M. F.:"Proc. of the 1995 Particle Accelerator Conf.", IEEE Inc., 1663 (1996).